



Characteristics and Production Technologies of Byzantine Building Bricks from the Anaia Church in Western Anatolia

Elif Çam · Elif Uğurlu Sağın

Accepted: 3 July 2023 / Published online: 4 August 2023
© The Author(s), under exclusive licence to The Clay Minerals Society 2023

Abstract Fired bricks were valued as essential building materials in the central tradition of Byzantine architecture in Constantinople (İstanbul), Anatolia, and the Balkans. In this study, Byzantine bricks from three construction periods, covering nearly nine centuries (fifth–fourteenth centuries), of Anaia Church (Kadıkalesi) in Western Anatolia were investigated to determine their characteristics, raw material properties, and production technologies. The characteristics of the bricks were evaluated and compared in order to identify similarities and differences between the periods and to investigate the continuity of the tradition of brick production over centuries. Basic physical and colorimetric properties, chemical and mineralogical compositions, thermal behavior, and microstructural and mechanical properties of bricks were determined by scanning electron microscopy (SEM) coupled with energy dispersive spectroscopy (SEM–EDS), Fourier-transform infrared spectrometry (FTIR), X-ray diffraction (XRD), thermogravimetric analysis (TGA), and mechanical tests. The results indicated that all the bricks in the Anaia Church were brown-beige colored, highly porous, low-density materials with low mechanical strength. They were produced from Ca-rich clays, probably obtained from two

different sources used during all construction periods. The mineralogical composition and thermal properties revealed that the bricks from the first and second periods were fired at between 800 and 900°C and the bricks from the third period were fired at <850°C. Greater calcium content and firing temperatures were found to reduce the total porosity and the number of small pores (<10 µm) and increase the mechanical strength of the bricks. The results of the study revealed no significant differences in the production of bricks, including raw material sources and kiln conditions, for the different construction periods of the church.

Keywords Anaia Church · Byzantine Period · Calcareous clays · Characterization · Firing temperature · Historical building bricks

Introduction

The characterization of historic brick materials, which are considered to reflect the knowledge and skills of their time, is crucial for the elucidation of ancient production technologies and for the conservation of historical buildings and archeological sites. The earliest known use of bricks, produced by molding a mixture of mud and straw, was in Mesopotamia in the eighth millennium BC (Bakırer, 1981; Wright, 2005). Mud bricks were used generally for small-scale structures such as houses; as larger-scale public buildings were

E. Çam (✉) · E. Uğurlu Sağın
Department of Conservation and Restoration of Cultural Heritage, İzmir Institute of Technology, 35430 Urla, İzmir, Türkiye
e-mail: elifcam@iyte.edu.tr

constructed over time, more weather-resistant materials were needed (Bakirer, 1981; Wright, 2009). In the fourth millennium BC, kiln-fired bricks were produced in Mesopotamia (Bakirer, 1981; Wright, 2009) and were used for structural elements exposed directly to moisture, such as foundations and lower parts of walls (Davey, 1961; Moorey, 1999). Kiln-fired bricks were introduced into Western architecture in the fourth century BC (Davey, 1961; Malacrino, 2010; Tucci, 2015) and became a primary building material during the Roman Empire (first century BC–fifth century AD) (Malacrino, 2010; Tucci, 2015). In Roman architecture, fired bricks were used in the construction of structural materials such as walls, arches, and domes, and also as facing materials for walls built with Roman concrete (Helen, 1975; Scalenghe et al., 2015; Tucci, 2015).

During the Byzantine Period (fourth–fifteenth centuries AD), fired bricks became the primary material for masonry construction, especially in Constantinople (İstanbul), Anatolia, and the Balkans. Brick masonry, therefore, was regarded as “the central tradition of Byzantine Architecture” (Mango, 1985). During the Byzantine period, the demand for brick production had increased and the use of many kilns at the same time became necessary, as construction work required thousands of bricks. For this reason, in the fourteenth century, a law called *Exbiblos* regulated the conditions for the location of the brick kilns, which, due to their large space requirements and air pollution, were located away from the cities and residential areas (Ousterhout, 1999).

Despite the changes in the utilization of fired bricks, their production methods remained similar over the centuries. The production process consisted of finding a suitable source of raw material, extracting the raw material, mixing it with water and sometimes additional materials, shaping, drying, and firing. During the process, the characteristics of the bricks changed according to the properties of the raw material and the stages of manufacturing (Benavente et al., 2006; Elert et al., 2003; Fernandes et al., 2010). The raw material and additives (straw, sand, old brick fragments, etc.) used in the production process affected the chemical and mineralogical compositions and the physical properties such as color, porosity, and pore structures (Cultrone et al., 2005; Davey, 1961; Pavia, 2006; Riccardi et al., 1999). The other important factor influencing porosity was the shaping method. Molding, which was the main method

used in the production of historic bricks, resulted in a greater total porosity than modern high-pressure methods (Carretero et al., 2002). Furthermore, firing, the final stage of production, caused significant physical and mineralogical changes.

Historical kilns for firing bricks generally consisted of two sections; the combustion chamber for lighting the fire and adding the fuel at the bottom, and the charging chamber at the top for the bricks to be fired (Adam, 2005; Davey, 1961; Wright, 2005). The heat distribution in these kiln systems was inhomogeneous as the temperature decreased toward the upper parts away from the fire. Thus, the bricks in the parts closest to the heat source were fired at temperatures that could reach almost 1000°C, gradually decreasing toward the top, while those furthest from the fire were fired at temperatures not exceeding 600°C, and even at ~450°C near the top (Adam, 2005; Davey, 1961; Scalenghe et al., 2015). Historical bricks were generally fired at lower temperatures (<900°C), and their density, strength, and durability were less than is the case for modern bricks, which are shaped under high pressure and fired at higher temperatures (>1000°C) (Benavente et al., 2006; Cultrone et al., 2004; Lopez-Arce & Garcia-Guinea, 2005; Uğurlu Sağın & Böke, 2013).

Previous studies on historical bricks have focused on the characterization and deterioration mechanisms of bricks used in different historical buildings, particularly from the Roman Period (Aslan Özkaya & Böke, 2009; Calliari et al., 2001; Lopez-Arce & Garcia-Guinea, 2005; Oguz et al., 2014; Scalenghe et al., 2015; Scatigno et al., 2018; Stefanidou et al., 2015; Uğurlu Sağın, 2017). However, the characteristics of the bricks from the Byzantine period have been subjected to relatively little study. In addition, recent research on the characterization of Byzantine bricks has focused mainly on the monuments from the center of the Empire, Constantinople (İstanbul) (Ballato et al., 2005; Bolognesi et al., 2004; Kahya, 1992; Kurugöl & Tekin, 2010; Moropoulou et al., 2002; Taranto et al., 2019; Ulukaya et al., 2017); and a limited number of studies exists on bricks used in the provinces (Eroğlu & Akyol, 2017; Kurugöl & Tekin, 2010; Özyıldırım & Akyol, 2016).

The aim of the current study was to determine the characteristics of building bricks from the Anaiia Church, Kadıkalesi in Western Anatolia, an important

provincial Byzantine religious building. The physical, microstructural, and mechanical properties, as well as the chemical and mineralogical compositions of bricks from three different construction periods of the church, dating from the fifth to the fourteenth century, were studied using various analytical methods. In particular, the results have been evaluated in order to elucidate the brick production techniques used in different centuries of Byzantium and its Anatolian provinces, and also to contribute to the conservation works to be carried out on the church.

Materials and Methods

In the present study, building bricks from the Anaia Church at the archeological site of Kadıkalesi in Kuşadası, Aydın, Turkey were investigated. The Anaia Church is located in a fortress named Kadıkalesi, on the Aegean coast, opposite the island of Samos (Fig. 1). The church was built as a monastery complex of the city of Anaia, which was a harbor city surrounding Kadıkalesi during the Byzantine Period (Mercangöz, 2005). Kadıkalesi was built on an alluvial plain surrounded by limestone (MTA, 2002).

The city is located close to the Büyük Menderes River (referred to historically as Maiandros) graben basin, which is characterized by modern and Quaternary deposits the lithofacial characteristics of which have been described as gravel (pebbly and unsorted), sand (gravelly, silty, shelly), and mud (sandy red, sandy grey, clayey red, clayey gray) (Kazancı et al., 2009). Kadıkalesi was known as one of the most important ceramic and glass production centers in the region during the Byzantine period. Recent findings, such as a pile of clay and a clay basin in the excavation site, indicate the use of clay and production of earthenware in Kadıkalesi (Mercangöz, 2013).

The Anaia Church had a three-naved plan with an apse, a substructure, inner and outer narthexes, cisterns, and baptisteries. The church, measuring 51.1 m × 27.5 m, was built in a masonry system, with stone-brick walls supported by buttresses. It was built in three phases, following the devastating earthquakes that occurred in different centuries (Mercangöz & Tok, 2011). The first construction period was between the fifth and sixth centuries. The naos ends with the apse and was built in this period on a substructure, and the baptistery in the north corner of the church was also thought to date from the same period (Hazinedar

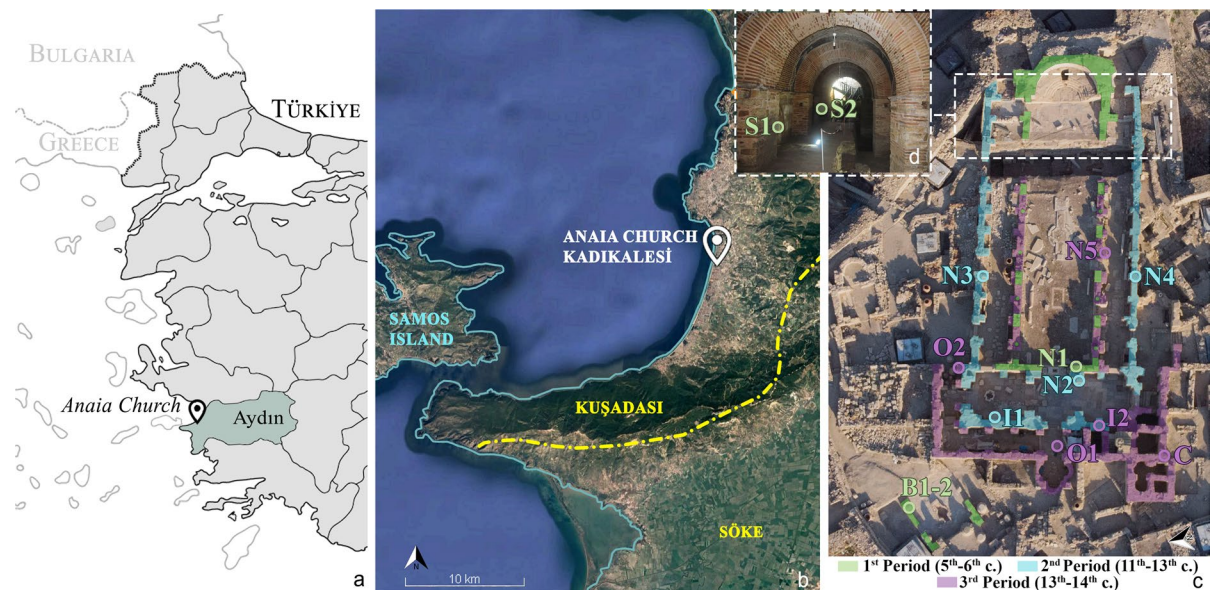


Fig. 1 a Map showing the location of the case study; b satellite image of Kuşadası showing the location of the case study (adapted from Google Earth); c aerial view of the Anaia Church, Kadıkalesi, showing the construction periods of the

church and the locations of samples (photo adapted from the Kadıkalesi Excavation Archive); and d photo (2021) of the substructure underneath the Anaia Church showing the sampling locations

Coşkun, 2021; Kanmaz & Ipekoğlu, 2016). After the earthquakes, probably in 1040 and 1056, both with a Mercalli intensity scale of VIII (Tepe et al., 2021), the piers and walls were added to the western and outer walls of the naos for consolidation, and the inner narthex was built in the second construction period, dated between the eleventh and thirteenth centuries. This was followed by the third construction period which took place between the thirteenth and fourteenth centuries (Kanzmaz & Ipekoğlu, 2016). During this period, new structures were built, such as the outer narthex, the cisterns, and the southern chapel. Measures were also taken to strengthen the building against earthquakes, including the addition of walls between the naves and buttresses to support the walls of the inner narthex (Kanzmaz & Ipekoğlu, 2016). The Anaia Church became an archbishopric in the thirteenth century. In addition, the city of Anaia gained the status of a commercial and customs center due to its geopolitical location (Foss, 1979; Mercangöz, 2007). In the fourteenth century, the Anaia Church was damaged structurally by an earthquake with an intensity of VII on the Mercalli scale (Tepe et al., 2021) and subsequently abandoned (Mercangöz & Tok, 2011).

In order to conduct the experimental part of the current study, 14 relatively sound brick samples were collected from the upper parts of the structural elements in order to avoid deterioration problems related to humidity. Sampling was carried out

in relation to the construction periods and spaces of the Church. Five bricks from the first and third construction periods and four bricks from the second period were taken without distinction as to their physical characteristics, such as color and size. The samples were labeled according to the spaces of the Church from which they were taken (B: Baptistery, C: Cistern, I: Inner Narthex, N: Naos, O: Outer Narthex, S: Substructure) (Fig. 1, Table 1).

The basic physical properties of the bricks were described in terms of their porosity, density, saturation coefficient, and pore interconnectivity values. Porosity, apparent density, and saturation coefficient were determined using the RILEM test methods (RILEM, 1980). Pore interconnectivity (A_x) was measured by using the saturated weights of the samples at atmospheric pressure (M_{atm}) and low pressure (M_{sat}). The equation used for calculating pore interconnectivity is given below (Eq. 1, Cultrone et al., 2004):

$$A_x = [(M_{sat} - M_{atm})/M_{sat}] \times 100 \quad (1)$$

Where A_x = Pore interconnectivity; M_{sat} = Saturated weights of samples at low pressure; and M_{atm} = Saturated weights of samples at atmospheric pressure

Colorimetric properties were defined according to the Munsell Soil Color Chart (Munsell Color (Firm) (2000)) and expressed in terms of hue, value, and chroma values. According to the Munsell Color

Table 1 List of samples and their locations

Sample		Location
1 st Construction Period (5 th –6 th c.)	B1	Baptistery—Rubble of the outer baptistery
	B2	Baptistery—Rubble of the outer baptistery
	S1	Substructure—Wall infill
	S2	Substructure—Buttress
	N1	Naos—Wall between naos and inner narthex
2 nd Construction Period (11 th –13 th c.)	N2	Naos—Buttress on the western wall
	N3	Naos—Buttress in the north aisle
	N4	Naos—Buttress in the southern aisle
	I1	Inner Narthex—Buttress
3 rd Construction Period (13 th –14 th c.)	I2	Inner Narthex—Wall infill
	C	Cistern—Wall
	N5	Naos—Wall between southern aisle and naos
	O1	Outer Narthex—Brick paving
	O2	Outer Narthex—Buttress

system, the hue represents color and is defined by five principles (R: Red, Y: Yellow, G: Green, B: Blue, P: Purple) and five intermediate colors (YR, GY, BG, PB, RP). In addition, the lightness of the color is expressed with values in the range of 0–10, from dark to light. The saturation color is indicated by chroma (Gerharz et al., 1988).

A scanning electron microscope (SEM) equipped with an X-ray energy dispersive system (EDS) (Quanta 250 FEG, FEI, Eindhoven, Netherlands) was used to determine the chemical compositions and microstructural properties of the bricks. Mineralogical compositions were determined by Fourier-transform infrared (FTIR) spectroscopy (Spectrum BX FTIR spectrometer, Perkin Elmer, Beaconsfield, UK) and X-ray diffraction (XRD) (Philips X-Pert Pro X-ray Diffractometer, Malvern Panalytical, Almelo, Netherlands) analyses. The fine brick powders were dispersed in pure KBr, and the mixture was pressed into pellets for FTIR analysis. The FTIR spectra were obtained in a wavenumber range from 4000 to 400 cm^{-1} with a resolution of 4 cm^{-1} . The XRD patterns of brick samples, ground finer than 53 μm , were obtained in the range 5–60°2 θ and at a scan speed of 1.6°2 θ per minute. *Panalytical Highscore Plus* software was used to determine the mineral phases exhibited in the XRD data. Weight losses of bricks at specific temperatures were measured using a Perkin Elmer Diamond TG/DTA instrument (Perkin Elmer, Boston, MA, USA). Standard abbreviations were used for mineral names as given by Kretz (1983) and Whitney and Evans (2010), and as supplemented by Warr (2020). Thermogravimetric analyses (TGA) were conducted on 8 of 14 samples, considering their chemical and mineralogical compositions. TGA was performed on brick powders (<53 μm) in a static nitrogen environment in the temperature range 25–1000°C at a rate of 10°C/min. The TGA results were evaluated in accordance with the mineralogical composition analyses, and the firing temperatures of the bricks were estimated.

The compressive strength and modulus of elasticity of bricks were used to define their mechanical properties. Samples were prepared in a cubic shape and ranged in size from 2 to 5 cm for compression tests. The force was applied to the samples at a speed of 0.5 mm/min using a Shimadzu AG-I mechanical test instrument (Shimadzu, Kyoto, Japan), the BS EN

772–1 + A1 procedure was followed for the mechanical analyses (European Standards, 2015).

Results and Discussion

Basic Physical Properties, Chemical Compositions, and Color Identifications of the Anaia Church Bricks and the Effect of the Manufacturing Process on the Properties

Basic physical properties of the Anaia Church bricks were defined by their apparent density (g/cm^3), total porosity (%), saturation coefficient, and pore interconnectivity values. Total porosity values of between 24.25 and 51.47% and apparent density values of between 1.22 and 1.73 g/cm^3 were measured (Table 2). B1, S1, and S2 from the first, N2 from the second, and N4 and I2 from the third construction periods were found to have the greatest porosity (49.78–51.47%) and lowest density (1.22–1.27 g/cm^3) values of all the samples. The bricks from the first construction period of the church were also found to have the greatest average porosity and the lowest average density (except for N1), while those from the third period had the lowest average porosity and the greatest average density.

Similar to the Anaia Church bricks, previous studies found that the historic bricks had high porosity and low-density values, probably because they were produced using similar molding methods and fired at low temperatures (Cardiano et al., 2004; Kahya, 1992; Tekin & Kurugöl, 2011; Ulukaya et al., 2017).

The saturation coefficient value is used to express the presence of large pores (>2 μm) in the material that are available to adsorb water; the value is considered to be an indication of resistance to freezing and thawing if it is <0.80 (ASTM C67–07, 2007). The coefficient was found to be between 0.84 and 0.94 for most of the samples from all the periods, and below 0.80 only for S2 from the first period and N4 from the second period (Table 2). This may be related to the greater proportion of large pores (>2 μm) in N4 and S2 than in other samples. Pore interconnectivity was also calculated; this refers to the interconnection between the pores enabled by microcracks and fissures and indicates the presence of pores where water is not easily accessible under natural conditions (Cultrone et al., 2004). The pore interconnectivity values

Table 2 Basic physical properties of the Anaia Church bricks

Sample		Porosity (%)	Apparent Density (g/cm ³)	Saturation Coefficient	Pore Interconnectivity
1 st Construction Period (5 th -6 th c.)	B1	49.8	1.3	0.85	4.27
	B2	41.2	1.4	0.89	2.65
	S1	51.5	1.2	0.89	3.28
	S2	50.4	1.3	0.77	6.47
	N1	24.2	1.7	0.84	2.08
2 nd Construction Period (11 th -13 th c.)	N2	51.3	1.3	0.89	3.25
	N3	36.3	1.5	0.92	1.53
	N4	38.9	1.5	0.70	6.09
	I1	38.5	1.5	0.89	2.11
3 rd Construction Period (13 th - 14 th c.)	I2	50.5	1.2	0.87	3.69
	N5	43.3	1.4	0.94	1.50
	C	33.3	1.5	0.92	1.59
	O1	29.9	1.7	0.89	1.76
	O2	31.3	1.6	0.91	1.52

of bricks increased when pores which water cannot reach under natural conditions increased in the material structure. As the cracks and fissures between the pores are lost due to vitrification at higher temperatures, it can be stated that the greater the pore interconnectivity value, the greater the degree of firing. Therefore, a larger pore interconnectivity value has been accepted as an indicator of greater resistance to salt crystallization and freeze-thaw cycles (Cultrone et al., 2004, 2005; Pérez-Monserrat et al., 2021). The pore interconnectivity values of the brick samples ranged from 1.50 to 6.47 (Table 2). The lowest average pore interconnectivity value was found in the bricks of the third construction period. The largest values were also determined in samples B1 (4.27) and S2 (6.47) of the first period, and N4 (6.09) of the second period (Table 2). Considering the parallel results of the saturation coefficient and the pore interconnectivity obtained in samples N4 and S2, these bricks can be stated to have been fired at higher temperatures than others.

The SEM-EDS analyses revealed that the bricks of the Anaia Church were composed of large amounts of SiO₂ (43.76–55.57 wt.%), Al₂O₃ (15.19–25.28 wt.%), and CaO (9.64–26.33 wt.%); moderate amounts of FeO (5.29–8.81 wt.%); and smaller amounts of MgO (1.98–5.29 wt.%), K₂O (2.97–4.29 wt.%), Na₂O (0.50–1.40 wt.%), and TiO₂ (0.46–0.87 wt.%) (Table 3). The main oxide

ratios of the Anaia Church bricks were in a similar range to the Byzantine bricks from the Kütahya and Trabzon fortifications (Kurugöl & Tekin, 2010) and the Hagia Sophia, Istanbul (Taranto et al., 2019).

Clays are generally classified according to their CaO values, as calcareous clays (or Ca-rich clays) if they contain >6% CaO, and non-calcareous clays (or Ca-poor clays) when they have <6% (Kumar Mishra et al., 2021; Maniatis & Tite, 1981; Moropoulou et al., 1995; Taranto et al., 2019). The major oxide compositions showed that the bricks of the Anaia Church were produced from calcareous clay sources, as their CaO content was >6%. The geological features of the region revealed that carbonates and clays were abundant in the surrounding area (Kazancı et al., 2009). Although the ancient sources of raw materials for the production of ceramics and bricks in the city of Anaia have not yet been found, it can be said that the immediate surroundings could have been the source of the raw materials.

Furthermore, two different ranges of CaO percentages were observed within the Anaia Church bricks, between 9.64–12.26% and 21.32–26.33%, regardless of the construction period. The three samples from the first period (B1, S1, S2) and two each from the second (N2, N4) and third (I2, N5) periods were the bricks with smaller CaO contents, while two samples from the first (B2, N1) and second (N3, I1) periods and three from the third

Table 3 Major oxide compositions (%) of bricks determined by SEM–EDS

Sample		SiO ₂	CaO	Al ₂ O ₃	FeO	MgO	K ₂ O	Na ₂ O	TiO ₂
1 st Period (5 th - 6 th c.)	B1	48.3	11.4	22.9	8.4	3.6	3.4	1.27	0.71
	B2	44.9	22.2	17.1	5.9	4.9	3.6	0.81	0.66
	S1	47.0	12.2	23.6	8.8	2.7	3.8	1.16	0.69
	S2	52.9	12.3	20.3	6.9	2.2	3.3	1.29	0.74
	N1	43.8	26.3	15.2	5.8	4.1	3.5	0.55	0.65
2 nd Period (11 th -13 th c.)	N2	48.9	9.7	25.3	8.5	2.2	3.5	1.40	0.55
	N3	45.0	25.0	15.2	5.7	4.9	3.0	0.78	0.46
	N4	55.6	9.6	19.6	7.7	2.0	3.6	1.24	0.63
	I1	43.9	23.6	16.0	5.3	5.3	4.2	1.11	0.63
3 rd Period (13 th -14 th c.)	I2	48.7	11.2	23.5	8.4	2.6	3.7	1.10	0.78
	N5	48.7	10.4	23.9	8.5	2.4	4.1	1.18	0.87
	C	43.9	21.3	18.1	6.4	4.7	3.9	0.91	0.70
	O1	43.8	22.3	16.6	6.1	5.1	4.3	1.00	0.74
	O2	43.8	23.8	16.4	6.4	4.9	3.5	0.50	0.73

period (C, O1, O2) were the bricks with greater CaO contents. This apparent difference in the chemical composition of the bricks may be due to the possibility that two different clays were used in the production of bricks in Anaia during the three construction periods of the Church.

The difference in CaO contents of the samples affected their basic physical properties. The samples with greater CaO contents had less porosity and greater density than others. The porosity and apparent densities of the samples with CaO > 20% were measured to be between 29.9–41.2% and 1.4–1.7 g/cm³, respectively, whereas the samples with lower CaO had porosity values between 38.9 and 52.7% and density between 1.2 and 1.5 g/cm³.















The chemical composition of the raw materials, together with the firing temperatures, determines the colorimetric properties of bricks. Calcium and iron oxides are the main causes of variations in brick colors from yellow/beige to red (Cultrone et al., 2005; Scatigno et al., 2018; Valanciene et al., 2010). The presence of Fe, mostly in the form of hematite, results in reddish colors of fired bricks (Pavia, 2006; Scatigno et al., 2018). Conversely, the yellowish color of bricks occurs in the presence of carbonates because they can inhibit the formation of iron oxides, which give a reddish color (Cultrone et al., 2005; Pavia, 2006; Pérez-Monserrat et al., 2022). The firing temperature affects the lightness values due to certain mineralogical transformations.

As the firing temperature increases, the color of Ca-rich bricks becomes lighter due to the formation of diopside (Cultrone et al., 2005; Rathossi & Pontikes, 2010), while Ca-poor bricks with large Fe contents have a darker red color (Pavia, 2006; Rathossi & Pontikes, 2010; Wang et al., 2023).

The colors of the Anaia Church bricks were determined using a Munsell Color Chart and the results were described as color codes with their hue, value, and chroma, as shown in Table 4. The hue of the samples was in a wide range of the red and yellow–red colors between 10R and 10YR, while the value was determined at between 6 and 8. Also, the chroma ranged between 3 and 6. Munsell Color tests showed that the majority of the bricks were brown-beige in color. No significant difference was found in the color of bricks between the construction periods. Samples with the smallest values, S2 from the first period, N2 and N4 from the second period, and I2 from the third period, had the darkest colors among the others (Table 4).

Although all the samples were found to be brown-beige in color due to the use of Ca-rich raw materials in their production, the bricks with larger CaO contents were also lighter in color than those with smaller CaO values. The darker colors of S2 (7.5YR/6/6), N2 (10R/6/6), N4 (7.5YR/6/3), and I2 (2.5YR/6/6) among the samples were caused by the formation of iron oxides, such as hematite and magnetite (Pavia, 2006; Tarhan & Işık, 2020), possibly due to firing at higher temperatures.

Table 4 Color of bricks determined using the Munsell Soil Color Chart

Sample	Hue	Value	Chroma	Color-code	Color	Color Name	
1 st Construction Period (5 th –6 th c.)	B1	2.5YR	7	4	2.5YR/7/4		Light Reddish Brown
	B2	7.5YR	8	4	7.5YR/8/4		Pink
	S1	2.5YR	7	6	2.5YR/7/6		Light Red
	S2	7.5YR	6	6	7.5YR/6/6		Reddish Yellow
	N1	5YR	8	4	5YR/8/4		Pink
2 nd Construction Period (11 th –13 th c.)	N2	10R	6	6	10R/6/6		Light Red
	N3	5YR	8	4	5YR/8/4		Pink
	N4	7.5YR	6	3	7.5YR/6/3		Light Brown
	I1	10YR	8	3	10YR/8/3		Very Pale Brown
3 rd Construction Period (13 th –14 th c.)	I2	2.5YR	6	6	2.5YR/6/6		Light Red
	N5	2.5YR	7	6	2.5YR/7/6		Light Red
	C	5YR	8	4	5YR/8/4		Pink
	O1	7.5YR	7	4	7.5YR/7/4		Pink
	O2	5YR	8	4	5YR/8/4		Pink

Mineralogical Compositions and Thermal Properties of the Anaia Church Bricks and Estimation of Firing Temperatures

Mineralogical compositions were determined via XRD and FTIR analyses. Mineralogical compositions were then evaluated to estimate firing temperatures.

The XRD analyses showed that the Anaia Church bricks were composed mainly of quartz (SiO₂), calcite (CaCO₃), albite (NaAlSi₃O₈), and muscovite (KAl₂(Si₂AlO₁₀)(OH)₂). The other mineral phases detected were hematite (Fe₂O₃), magnetite (Fe₃O₄), gehlenite (Ca₂Al₂SiO₇), anorthite (CaAl₂Si₂O₈), diopside (CaMgSi₂O₆), and dolomite (CaMg(CO₃)₂) (Fig. 2, Table 5).

In the FTIR spectra, the O–H stretching peaks at 3422–3448 cm⁻¹ and H–O–H bending peaks at 1630–1645 cm⁻¹ were detected in all samples, indicating absorbed water within the brick structure (Fig. 3, Table 6). The peaks of the C–H stretching mode in the range 2924–2934 cm⁻¹, associated with organic matter, were very weak in B2, N1, I2, N5, O1, and O2 samples (Maritan et al., 2006; Şerifaki, 2017; Şerifaki, 2017; Stuart, 2007;). The most characteristic peaks between 1022 and 1084 cm⁻¹, detected in all samples (Fig. 3, Table 6) were attributed to the Si–O stretching mode of quartz (Maritan et al.,

2006; Uğurlu Sağın, 2017). Other quartz peaks were detected as doublets at 796–798 and 774–779 cm⁻¹ (De Benedetto et al., 2002; Gadsden, 1975), as single peaks at 691–695 and 503–514 cm⁻¹ (Gadsden, 1975), and as Si–O–Si symmetric bending at 456–485 cm⁻¹ (Hlavay et al., 1978). Calcite, which was found in most of the bricks, was identified by peaks at 713–714 cm⁻¹, 874–876 cm⁻¹ as a shoulder, and in the (CO₃)²⁻ stretching mode at 1430–1455 cm⁻¹ (Gadsden, 1975; Maritan et al., 2006; Uğurlu Sağın, 2017). Furthermore, the absorption bands in the region 2514–2517 cm⁻¹ and 1793–1797 cm⁻¹, which are associated with calcite (Demir et al., 2018; Gadsden, 1975), were observed only in samples with CaO contents of >20%. Triplet peaks of anorthite in the regions of 621–622, 574–584, and 530–540 cm⁻¹ were present in the spectra of the N2, N4, and S2 samples (Gadsden, 1975) (Fig. 3, Table 6). Peaks at 647–648 cm⁻¹ were also assigned to albite (Chukanov, 2014; Gadsden, 1975).

The weight losses of the brick samples due to temperature changes were determined by TGA (Fig. 4 and Table 7). The total weight loss of the bricks between 25 and 1000°C was between 1.30 and 16.91%. The samples with smaller CaO values (S2, N4, and I2) demonstrated smaller weight losses (1.30–5.51%) compared to others (Fig. 4, Table 7).

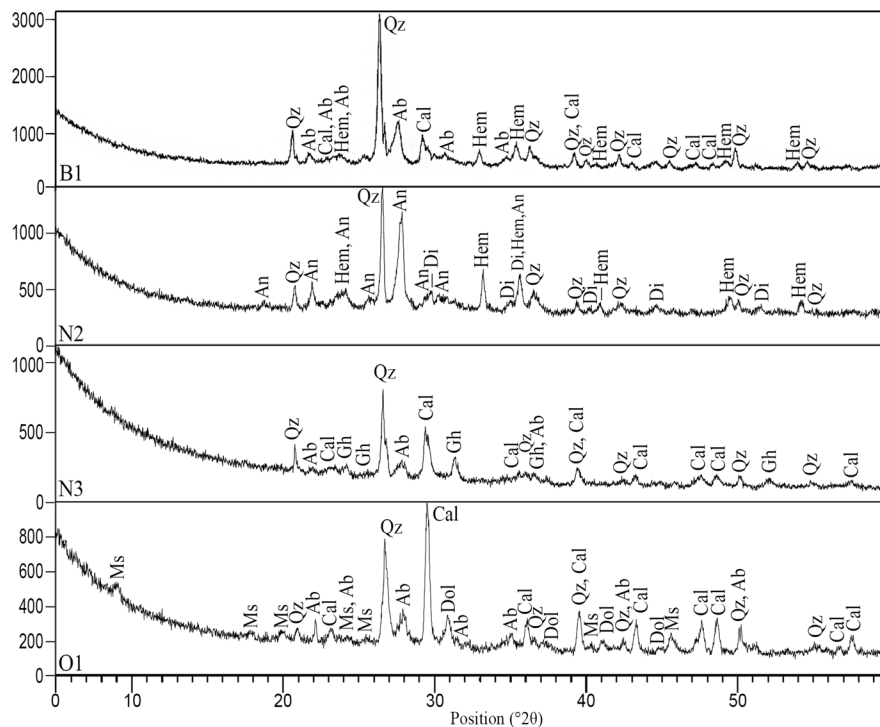


Fig. 2 XRD patterns of the Anaia Church bricks (samples B1, N2, N3, O1) (Ab: Albite, An: Anorthite, Cal: Calcite, Di: Diopside, Dol: Dolomite, Gh: Gehlenite, Hem: Hematite, Ms: Muscovite, Qz: Quartz)

In the thermal behavior of fired bricks, the weight losses between 25 and 400°C are associated with removal of water from the brick structures, whereas weight losses between 25 and 100°C are due to physically adsorbed water, and losses between 100 and 400°C are due to the dehydration of bound water (Cardiano et al., 2004; Drebushchak et al., 2005; Paama et al., 2000; Singh & Sharma, 2016). Between 400 and 600°C, weight losses occur due to dehydroxylation (Cardiano et al., 2004; Drebushchak et al., 2005; Stubňa & Podoba, 2013), and oxidation of organic compounds results in weight losses in the range 200–600°C (Kumar Mishra et al., 2021; Ramachandran et al., 2002; Singh & Sharma, 2016).

For the Anaia Church bricks, weight losses of 0.05–1.43% were measured up to 100°C, and dehydration resulted in a weight loss of 1.09–3.98% between 100 and 400°C (Fig. 4, Table 7). Weight loss between 400 and 600°C due to dehydroxylation and oxidation of organic matter ranged from 0.28 to 3.04% (Table 7). In addition, the sharp decrease observed around 600°C in the I2 (2.01%) and N4

(0.57%) samples was attributed to the phase transformation of quartz (α - β transformation) (Ion et al., 2011) (Fig. 4).

The largest weight losses (6.61–12.88%) were observed at ~700°C in N1, N3, I1, C, and O1 (Fig. 4). The decomposition of carbonates was assumed to be responsible for the weight losses between 700 and 800°C (Cardiano et al., 2004; Drebushchak et al., 2005; Paama et al., 2000; Singh & Sharma, 2016). Considering the large CaO contents in N1, N3, I1, C, and O1 (21.32–26.33%), the weight losses in this temperature range can be explained by calcite decomposition.

The mineralogical compositions and thermogravimetric analyses of the Anaia Church bricks were used to estimate their firing temperatures because the firing caused mineralogical changes in the raw materials of the bricks. During heating, kaolinite decomposed at 550°C (Cultrone et al., 2001; El Ouahabi et al., 2015). Furthermore, calcite, which is commonly found in calcareous bricks, begins to decompose at 800°C and disappears at ~870°C (Cultrone et al., 2004). Calcite

Table 5 Mineral phases of the Anaia Church bricks detected by XRD

Samples	Minerals									
	Qz	Cal	Ab	Ms	Hem	Gh	An	Di	Dol	Mag
B1	X	X	X		X					
B2	X	X	X	X		X				
S1	X	X		X	X	X				
S2	X				X		X	X		
N1	X	X	X	X						
N2	X				X		X	X		
N3	X	X	X			X				
N4	X						X	X		X
I1	X	X							X	
I2	X	X		X	X	X				
N5	X	X		X						
C	X	X	X	X						
O1	X	X	X	X					X	
O2	X	X	X	X		X				

Qz – Quartz, Cal – Calcite, Ab – Albite, Ms – Muscovite, Hem – Hematite, Gh – Gehlenite, An – Anorthite, Di – Diopside, Dol – Dolomite, – Mag Magnetite

decomposition is an irreversible structural change; therefore, the presence of calcite may indicate firing below 850°C (Drebushchak et al., 2005; Stubňa & Podoba, 2013). The mica group minerals, illite and muscovite, can be observed up to 900°C (El Ouahabi et al., 2015; Gliozzo, 2020; Scatigno et al., 2018). These decomposed minerals, calcite, dolomite, illite, and muscovite, underwent reactions at higher temperatures to form new mineral phases. Gehlenite forms as a reaction product of calcite and illite at ~800°C, and remains up to 1000°C (Cardiano et al., 2004; Cultrone et al., 2001; Pérez-Monserrat et al., 2021). In addition, quartz and dolomite react in calcareous bricks, and diopside forms at 900°C and disappears at 1100°C (Cardiano et al., 2004; Gliozzo, 2020; Pérez-Monserrat et al., 2021). Furthermore, albite starts to change phase at temperatures > 900°C (Riccardi et al., 1999; Tekin & Kurugöl, 2011), while anorthite occurs at 850°C (Cardiano et al., 2004; Uğurlu Sağın, 2017). The presence of hematite is another indication that the firing temperature was > 850°C, as it begins to form at this temperature (Cardiano et al., 2004; Uğurlu Sağın & Böke, 2013). Quartz, one of the primary minerals in bricks, exists at up to 1000°C, and is transformed into cristobalite above this temperature

(El Ouahabi et al., 2015). Wollastonite and spinel occurring above 900°C and mullite forming above 1000°C are the other indicators of high firing temperatures (El Ouahabi et al., 2015; Pavia, 2006).

The mineral content and weight loss of the Anaia Church bricks indicated that their firing temperatures were in the range of 800–900°C. N1, I1, N5, C, and O1 samples contained no mineral phases produced by temperature increase, e.g. gehlenite, which forms at 800°C, and anorthite or hematite, which appear at ~850°C. They contained calcite and muscovite (except I1), which disappear at ~870 and 900°C, respectively (Table 5). The TGA results also showed that the greatest losses (7.25–12.88%) in these samples were due to the decomposition of carbonates at ~700°C (Fig. 4). The absence of gehlenite, the presence of calcite and muscovite, and the large weight losses due to carbonates suggested that the firing temperatures of N1, I1, N5, C, and O1 did not exceed 800°C.

B2, N3, and O2 samples were composed of quartz, calcite, albite, and gehlenite. The presence of gehlenite indicated that their firing temperature exceeded 800°C, whereas the absence of hematite and anorthite indicated that their firing temperature did not reach

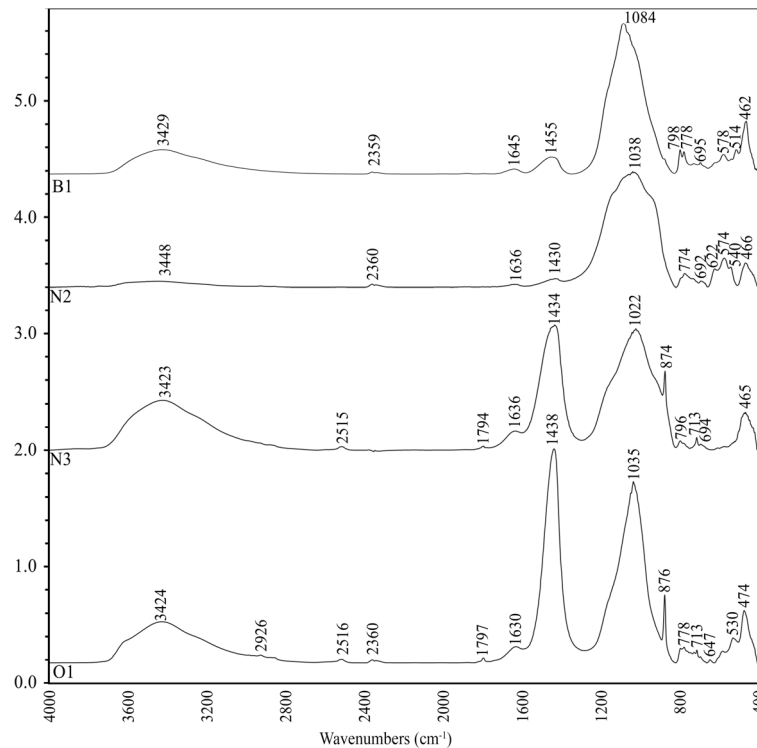


Fig. 3 FTIR spectra of the Anaia Church bricks (samples B1, N2, N3, O1)

850°C (Table 5). According to the TGA (N3), carbonates caused the sample to lose 6% of its weight (Fig. 4), suggesting that the firing temperature was ~800°C.

Hematite identified in B1, S1, and I2 indicated firing temperatures of >850°C. In addition, calcite, which decomposes at 870°C, was observed in these samples, and it was associated with a weight loss of 1.53% in sample I2. Therefore, the firing temperatures for samples B1, S1, and I2 were estimated to be between 850 and 870°C.

Samples S2, N2, and N4 were the only samples containing anorthite and diopside. Thus, the highest firing temperatures for these three samples were estimated to be ~900°C. Calcite peaks observed in the FTIR spectra of N4 (Table 6) indicated that it may have been fired at a temperature not exceeding 900°C.

The total weight loss of the bricks is assumed to be related to the firing temperatures; bricks fired at lower temperatures lose more weight than those fired at higher temperatures (Kumar Mishra et al., 2021). Accordingly, the TGA results showed that the greatest weight losses (13.4–16.9%) were recorded for bricks

for which the firing temperatures were estimated to be <800°C (N1, I1, C, and O1). The smallest weight losses (1.3–2.5%) were determined for the bricks fired at ~900°C (S2 and N4) (Table 7).

The comparison between the construction periods showed that the firing temperatures of samples from the third period (thirteenth–fourteenth centuries) were smaller than those of the first (fifth–sixth centuries) and second (eleventh–thirteenth centuries) periods. The bricks from the first and second periods were fired at temperatures ranging from <800 to 900°C. Conversely, none of the samples from the third period was fired at a temperature of >850°C. There is no information about the kilns in which the bricks were made at Anaia and whether production continued in the same kilns over the centuries, covering the different periods of construction of the Church. Therefore, it would be speculative to suggest that the bricks used in the third construction period were produced in a different kiln, considering that the inhomogeneous heat distribution of the ancient brick kilns used during the Byzantine Period could also be the reason for the aforementioned differences.

Table 6 Functional groups and their vibrational wavenumbers (cm⁻¹) determined in FTIR spectra of the Anaia Church bricks

Vibrational wavenumbers (cm ⁻¹)	3422–3448	2924–2934	2514–2517	1793–1797	1630–1645	1432–1455	1022–1084	874–876	796–798	774–778	713–714	692–695	647–648	621–622	574–584	530–540	511–514	456–485		
Peak characteristics	O–H stretching of absorbed water	Aliphatic C–H stretching of organic matter	Calcite	Calcite	H–O–H bending of absorbed water	(CO ₃) ²⁻ stretching of Calcite	Si–O stretching of Quartz	Calcite	Symmetrical stretching of Quartz	Si–O stretching of Quartz	Calcite	Quartz	Albite	Anorthite	Si–O–Al stretching of Anorthite	triplet	triplet	shoulder		
Minerals			Calcite	Calcite				Calcite			Calcite	Quartz	Albite	Anorthite	Si–O–Al stretching of Anorthite	triplet	triplet	shoulder	Quartz	
Samples																				Quartz
B1	3429				1645	1455	1084		798	778		695					514			462
B2	3423	2940	2516	1793	1637	1433	1027	874	796		713	693								464
S1	3438				1637	1438	1038			778		693								484
S2	3437	2925	2514	1795	1639	1430	1078	875	797	778	713	695		621	584	536	511			461
N1	3422				1636	1430	1030			777		692		622	574	540				472
N2	3448				1636	1434	1038	874	796	774	713	694								466
N3	3423		2515	1794	1636	1434	1022	874	796			694								465
N4	3460				1630	1434	1076	875	796	777		694		622	575	539				466
I1	3422		2517		1638	1427	1029	875	800		713									473
I2	3424	2926			1639	1438	1050	876	796	778	713	694								483
N5	3423	2934			1638	1438	1038	876	797	778	713	695								472
C	3434		2514	1796	1638	1434	1037	876		778	713		648							479
O1	3424	2926	2516	1797	1630	1438	1035	876		778	713		647			530				474
O2	3423	2927	2515		1639	1438	1025	876		778	714									456

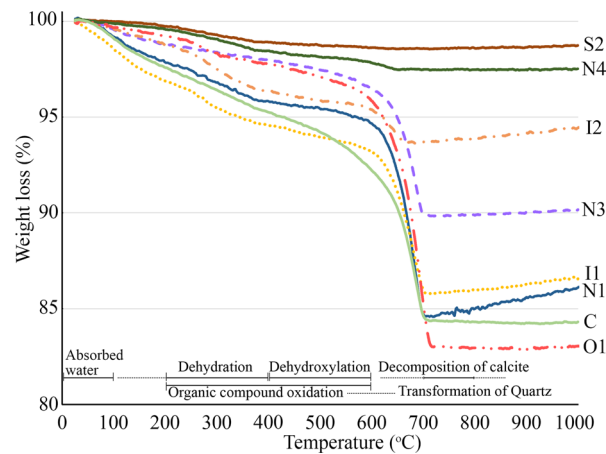


Fig. 4 TGA graphs of the Anai Church bricks

Microstructural Properties

Microstructural properties help to reveal the degree of vitrification, porosity, and pore characteristics of bricks. The microstructure of bricks fired at low temperatures is distinguished by a flaky structure with layered phyllosilicates, scattered particles, and angular pores between the grains (Cultrone et al., 2004, 2005; Maniatis & Tite, 1981; Pavia, 2006). At higher temperatures (800–870°C), calcite decomposition causes an increase in porosity in calcareous bricks (Buchner et al., 2021; Elert et al., 2003). However, glassy phases are not observed until temperatures reach 900°C, and above 900°C, the sharp-edged structures of phyllosilicates are deformed and smoothed as vitrification increases (Cultrone et al., 2004; Pavia, 2006; Pérez-Monserrat et al., 2022). Also, angular pores are still present at ~900°C, whereas higher temperatures lead to the formation of

ellipsoidal pores without interconnections (Benavente et al., 2006; Cultrone et al., 2001).

In the SEM images of N5 and O1, which were the samples fired below 800°C, crystalline structures and lamellar phyllosilicates were found. No glassy phases were observed in their matrix, and small pores (<10 µm) with irregular and angular shapes were identified (Fig. 5a, b). Furthermore, the microstructure and pore shapes of S1 (~850°C), and B2 (800–850°C) were similar to those of N5 and O1. However, the pore size (10–20 µm) and porosity were larger than those of bricks fired at up to 800°C, probably due to the decomposition of calcite which begins above 800°C (Fig. 5c, d). The absence of vitrification and angular pore characteristics in samples B2, N3, O1, and S1 showed that their firing temperatures did not exceed 900°C.

On the other hand, a glassy phase together with a crystalline phase was observed in S2 due to firing

Table 7 Weight losses (%) over various temperature ranges

Sample	25–200°C	200–400°C	400–600°C	600–800°C	800–1000°C	Total
S2	0.31	0.83	0.28	0.04	-0.15	1.30
N1	2.17	2.03	1.17	9.65	-1.17	13.90
N3	1.26	0.81	1.49	6.61	-0.29	9.88
N4	0.42	1.11	0.64	0.35	-0.05	2.48
I1	3.10	2.30	1.39	7.25	-0.65	13.38
I2	1.16	2.42	0.98	1.53	-0.59	5.51
C	2.44	2.34	3.04	7.89	0.00	15.71
O1	0.74	1.46	1.94	12.88	-0.10	16.91

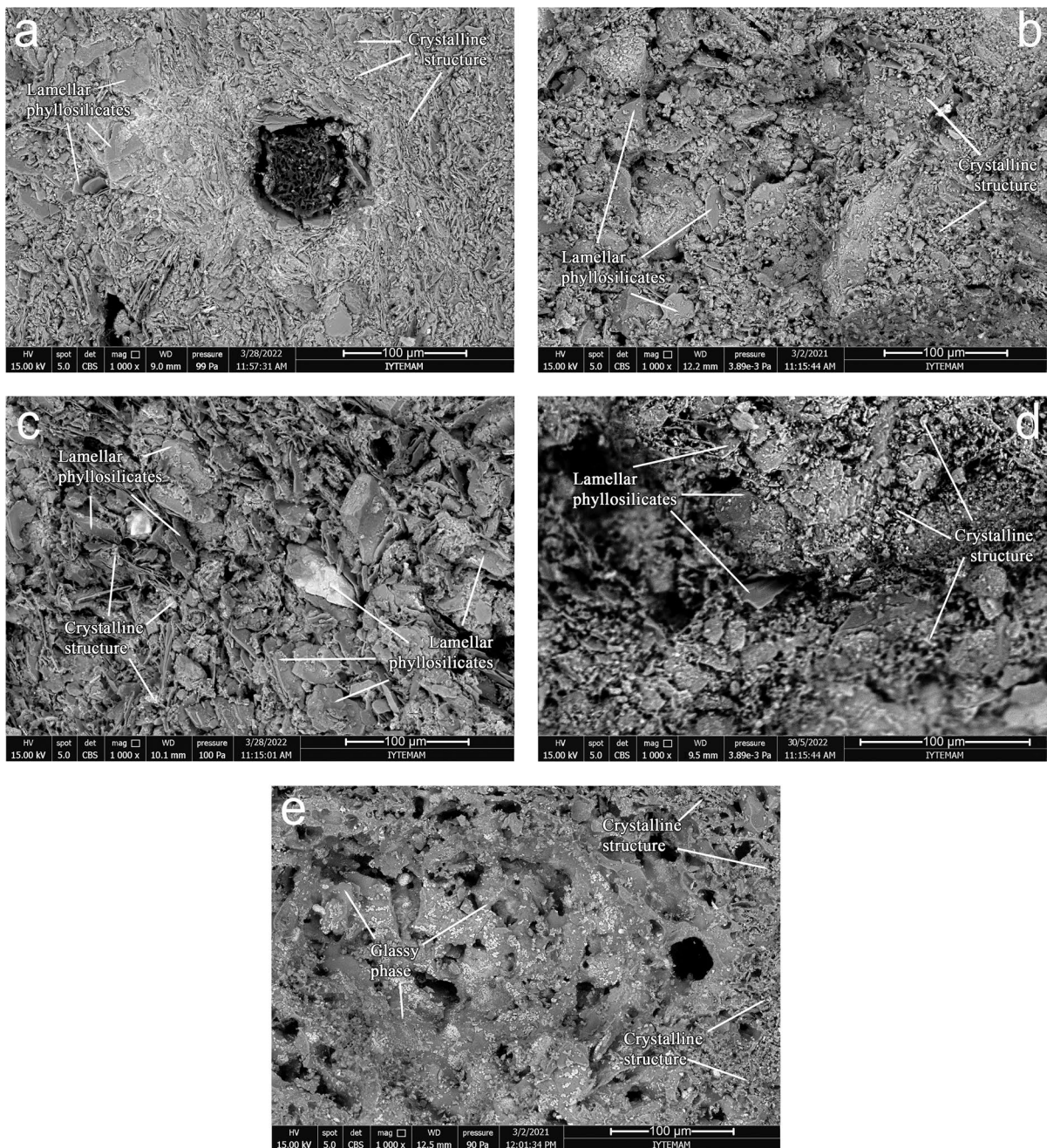


Fig. 5 SEM images of samples **a** N5 (CaO: 10.45%, < 800°C), **b** O1 (CaO: 22.33%, < 800°C), **c** S1 (CaO: 12.21%, ~850°C), **d** B2 (CaO: 22.16%, 800–850°C), **e** S2 (CaO: 12.26%, ~900°C)

at ~900°C. The higher temperature affected the pore structure of the bricks. The pores of S2, with ellipsoidal shapes, had larger sizes (<40 µm) because the micropores within the bricks were filled and merged as a result of melting (Fig. 5e).

The pore interconnectivity and saturation coefficient values demonstrated the relationship between pore structure and firing temperature. S2 and N4, the samples estimated to have been fired at higher temperatures (~900°C) than the others, had the highest

pore interconnectivity and the lowest saturation coefficient values (<0.8) among the Anaia Church bricks. These results indicated that the amount of micropores and the interconnection between the pores of the bricks decreased with the effect of firing at $\sim 900^\circ\text{C}$. Larger pores ($>2\ \mu\text{m}$) induced by higher firing temperatures would make the bricks more resistant to salt crystallization as the crystallization pressure inside the larger pores would be lower (Elert et al., 2003; Scherer, 1999), and resistant also to the freeze–thaw cycles as they would ensure that the trapped air was compressed (Bellanger et al., 1993; Elert et al., 2003). The inference, therefore, is that the bricks fired at $\sim 900^\circ\text{C}$ would be more resistant to salt crystallization and freeze–thaw cycles than those fired at lower temperatures.

Mechanical Properties

The uniaxial compressive strength and modulus of elasticity values were determined to evaluate the mechanical properties of the Anaia Church bricks (Table 8). Anaia Church bricks had a low uniaxial compressive strength (4.8–24.5 MPa) and modulus of elasticity (89–771 MPa). The compressive strength of bricks from the first construction period varied between 5.8 and 24.5 MPa, and those of bricks from

the third period varied between 4.8 and 19.9 MPa. The compressive strength values of the bricks belonging to the second construction period varied in a narrower range compared to the first and third periods, and the values were determined to be between 11.0–16.4 MPa.

The modulus of elasticity values were consistent with the compressive strength values. They varied between 143 and 771 MPa in the first period, between 321 and 486 MPa in the second period, and between 89 and 588 MPa in the third period. The results showed that mechanical properties did not differ among the construction periods. The variations in mechanical strength values were also found in Byzantine bricks from Greece (4.5–16.1 MPa (Stefanidou et al., 2015)) and Turkey (8.7–34.7 MPa (Kahya, 1992) and 7.9–33.0 MPa (Kurugöl & Tekin, 2010)). The ancient mixing and shaping process caused the uneven distribution and size of the pores and particles in the brick structure, resulting in a wide range of strength values in historic bricks (İspir, 2010; Kahya, 1992).

Compressive strength and total porosity are correlated, and bricks with lower porosity have greater compressive strength (Elert et al., 2003; Wang et al., 2023). The sample with the greatest compressive strength and modulus of elasticity was N1 from the first period ($<800^\circ\text{C}$) (Table 8). It was the sample with the lowest porosity (24.25%), the greatest density ($1.73\ \text{g/cm}^3$), and the largest CaO content (26.33%) among the samples. However, this clear correlation between strength and porosity was not observed for the other samples. In this case, it was the firing temperature and the CaO content that were found to be more influential in terms of the mechanical properties. Increasing the firing temperature improved the mechanical strength of the samples. The compressive strength of bricks with a CaO content of $<20\%$ was measured at between 11.0 and 16.4 MPa for bricks fired at 900°C and between 5.8 and 9.3 MPa for those fired at up to 850°C (Table 9). For bricks with a CaO content of $>20\%$, firing between 800 and 850°C resulted in compressive strength values of 12.9–19.9 MPa, while for bricks fired at $<800^\circ\text{C}$ it was measured to be between 4.8 and 11.9 MPa (excluding N1(24.5 MPa)) (Table 9). Similarly, a larger CaO content promoted compressive strength at lower firing temperatures compared to bricks with smaller CaO contents.

Table 8 Uniaxial compressive strength and modulus of elasticity values of the Anaia Church bricks

Sample	Uniaxial Compressive Strength (MPa)	Modulus of Elasticity (MPa)
1 st Period (5 th - 6 th c.)	B1	7.9
	B2	14.7
	S1	5.8
	S2	11.2
	N1	24.5
2 nd Period (11 th - 13 th c.)	N2	11.0
	N3	12.9
	N4	16.4
	I1	11.5
3 rd Period (13 th - 14 th c.)	I2	9.3
	C	11.9
	N5	5.9
	O1	4.8
	O2	19.9

Table 9 The comparisons among CaO content, compressive strength, and estimated firing temperatures of the Anaia Church bricks

Sample		Estimated firing temperature (°C)	Compressive strength (MPa)
CaO: <20%	N4	~900	16.4
	S2	~900	11.2
	N2	~900	11.0
	I2	~850	9.3
	B1	~850	7.9
	S1	~850	5.8
CaO: >20%	N5	<800	5.9
	O2	800–850	19.9
	B2	800–850	14.7
	N3	800–850	12.9
	N1	<800	24.5
	C	<800	11.9
	I1	<800	11.5
O1	<800	4.8	

Conclusions

The Anaia Church, one of the most important historical religious centers in Western Anatolia, is an outstanding example of Byzantine architecture built in the provinces of the Empire. It was built in masonry with natural stones and kiln-fired bricks. The Church was first built in the fifth century and, after devastating earthquakes in the region, it was consolidated, partly reconstructed, and extended with new spaces between the eleventh–thirteenth and thirteenth–fourteenth centuries.

All the bricks of the Anaia Church, from three phases of construction, were of a brown-beige color, low-density, and high-porosity. They had small values for uniaxial compressive strength and modulus of elasticity, regardless of the construction period. The bricks were manufactured from calcareous clay sources composed of large amounts of SiO₂, Al₂O₃, and CaO, with moderate amounts of FeO. The CaO content of the bricks ranged between 9.64–12.26% and 21.32–26.33%, suggesting the possibility that two different raw material sources were used during the three construction periods. All of the bricks were composed mainly of quartz, calcite, albite, and muscovite. The first- and second-period bricks were fired at between 800 and 900°C, while the third-period bricks were fired at <850°C.

A large CaO content and low firing temperatures affected their physical and microstructural properties. Lighter colors were observed in the bricks with a larger carbonate content (>20%) and fired at temperatures of 800°C, while the temperatures above 850°C produced darker colors in the bricks with a smaller Ca content (<20%). As the firing temperatures increased, the total porosity decreased, smaller pores (<10 µm) began to disappear, and the interconnections between pores decreased due to vitrification. In addition, a larger carbonate content was found to improve mechanical strength at low firing temperatures.

This study has shown that brick production in Western Anatolia during the Byzantine period continued for about nine centuries with similar raw material sources and production techniques. Possible sources of raw materials should be investigated in the vicinity of the Büyük Menderes graben, an area rich in clay, and, in particular, the settlement of Anaia (Kadikalesi). Comparison of the major- and trace-element compositions of possible raw material sources with the bricks in the Anaia Church, using statistical methods, will shed light on the history of Anaia and contribute to conservation studies.

Acknowledgements The authors thank Prof. Dr Zeynep Mercangöz and the Kadikalesi/Anaia excavation team for their support and guidance. They also thank the Centre for Materials Research at Izmir Institute of Technology for SEM-EDS, XRD, and TGA analyses.

Funding This study was supported by B-type Scientific Research Project Funding of IZTECH (No: 2021IYTE-1-0080), in compliance with the M.Sc. thesis entitled ‘Characteristics of Byzantine Period Building Bricks Used in St. Jean Basilica (Ayasuluk Hill) and Anaia Church (Kadikalesi)’ prepared by Elif Çam under the supervision of Elif Uğurlu Sağın.

Data Availability Data sets from the study are available upon request from the corresponding author.

Declarations

Conflict of Interest The authors declare that they have no conflict of interest.

References

- Adam, J.-P. (2005). *Roman Building: Materials and Techniques*. Routledge.
- Aslan Özkaya, Ö., & Böke, H. (2009). Properties of Roman bricks and mortars used in Serapis temple in the city of Pergamon. *Materials Characterization*, 60(9), 995–1000. <https://doi.org/10.1016/j.matchar.2009.04.003>

- ASTM C67–07. (2007). *Standard test methods for sampling and testing brick and structural clay tile*. ASTM International, PA, USA.
- Bakırer, Ö. (1981). *Selçuklu Öncesi ve Selçuklu Dönemi Anadolu Mimarisinde Tuğla Kullanımı*. Middle East Technical University.
- Ballato, P., Cruciani, G., Dalconi, M. C., Fabbri, B., & Macchiarola, M. (2005). Mineralogical study of historical bricks from the Great Palace of the Byzantine Emperors in Istanbul based on powder X-ray diffraction data. *European Journal of Mineralogy*, 17(5), 777–784. <https://doi.org/10.1127/0935-1221/2005/0017-0777>
- Bellanger, M., Homand, F., & Remy, J. M. (1993). Water behaviour in limestones as a function of pores structure: Application to frost resistance of some Lorraine limestones. *Engineering Geology*, 36, 99–108. [https://doi.org/10.1016/0013-7952\(93\)90022-5](https://doi.org/10.1016/0013-7952(93)90022-5)
- Benavente, D., Linares-Fernández, L., Cultrone, G., & Sebastián, E. (2006). Influence of microstructure on the resistance to salt crystallisation damage in brick. *Materials and Structures/Materiaux Et Constructions*, 39(1), 105–113. <https://doi.org/10.1617/s11527-005-9037-0>
- Bolognesi, E., Fabbri, B., Macchiarola, M., & Kotas, P. (2004). Characterisation of Historic Bricks from the Ruins of the Great Imperial Palace in Istanbul. *Key Engineering Materials*, 264–268(III), 2383–2386. <https://doi.org/10.4028/WWW.SCIENTIFIC.NET/KEM.264-268.2383>
- Buchner, T., Kiefer, T., Gaggli, W., Zelaya-Lainez, L., & Füssl, J. (2021). Automated Morphometrical Characterization of Material Phases of Fired Clay Bricks Based on Scanning Electron Microscopy, Energy Dispersive X-ray Spectroscopy and Powder X-ray Diffraction. *Construction and Building Materials*, 288, 122909. <https://doi.org/10.1016/J.CONBUILDMAT.2021.122909>
- Calliari, I., Canal, E., Cavazzoni, S., & Lazzarini, L. (2001). Roman bricks from the Lagoon of Venice: A chemical characterization with methods of multivariate analysis. *Journal of Cultural Heritage*, 2, 23–29.
- Cardiano, P., Ioppolo, S., De Stefano, C., Pettignano, A., Sergi, S., & Piraino, P. (2004). Study and characterization of the ancient bricks of monastery of “San Filippo di Fragalà” in Fraxzanò (Sicily). *Analytica Chimica Acta*, 519(1), 103–111. <https://doi.org/10.1016/j.aca.2004.05.042>
- Carretero, M. I., Dondi, M., Fabbri, B., & Raimondo, M. (2002). The influence of shaping and firing technology on ceramic properties of calcareous and non-calcareous illitic-chloritic clays. *Applied Clay Science*, 20(6), 301–306. [https://doi.org/10.1016/S0169-1317\(01\)00076-X](https://doi.org/10.1016/S0169-1317(01)00076-X)
- Chukanov, N. V. (2014). *Infrared spectra of mineral species*. Springer. <https://doi.org/10.1007/978-94-007-7128-4>
- Cultrone, G., Rodriguez-Navarro, C., Sebastian, E., Cazalla, O., & De La Torre, M. J. (2001). Carbonate and silicate phase reactions during ceramic firing. *European Journal of Mineralogy*, 13(3), 621–634. <https://doi.org/10.1127/0935-1221/2001/0013-0621>
- Cultrone, G., Sebastián, E., Elert, K., de la Torre, M. J., Cazalla, O., & Rodriguez-Navarro, C. (2004). Influence of mineralogy and firing temperature on the porosity of bricks. *Journal of the European Ceramic Society*, 24(3), 547–564. [https://doi.org/10.1016/S0955-2219\(03\)00249-8](https://doi.org/10.1016/S0955-2219(03)00249-8)
- Cultrone, G., Sidraba, I., & Sebastián, E. (2005). Mineralogical and physical characterization of the bricks used in the construction of the “Triangul Bastion”, Riga (Latvia). *Applied Clay Science*, 28, 297–308. <https://doi.org/10.1016/j.clay.2004.02.005>
- Davey, N. (1961). *A History of Building Materials*. Phoenix House Publication.
- De Benedetto, G. E., Laviano, R., Sabbatini, L., & Zambonin, P. G. (2002). Infrared spectroscopy in the mineralogical characterization of ancient pottery. *Journal of Cultural Heritage*, 3, 177–186.
- Demir, S., Şerifaki, K., & Böke, H. (2018). Execution technique and pigment characteristics of Byzantine wall paintings of Anaia Church in Western Anatolia. *Journal of Archaeological Science: Reports*, 17, 39–46. <https://doi.org/10.1016/J.JASREP.2017.09.037>
- Drebushchak, V. A., Mylnikova, L. N., Drebushchak, T. N., & Boldyrev, V. V. (2005). The investigation of ancient pottery: Application of thermal analysis. *Journal of Thermal Analysis and Calorimetry*, 82(3), 617–626. <https://doi.org/10.1007/S10973-005-0942-9>
- El Ouahabi, M., Daoudi, L., Hatert, F., & Fagel, N. (2015). Modified Mineral Phases During Clay Ceramic Firing. *Clays and Clay Minerals*, 63, 404–413. <https://doi.org/10.1346/CCMN.2015.0630506>
- Elert, K., Cultrone, G., Rodriguez-Navarro, C., & Sebastián Pardo, E. (2003). Durability of bricks used in the conservation of historic buildings - Influence of composition and microstructure. *Journal of Cultural Heritage*, 4(2), 91–99. [https://doi.org/10.1016/S1296-2074\(03\)00020-7](https://doi.org/10.1016/S1296-2074(03)00020-7)
- Eroğlu, M., & Akyol, A. A. (2017). Antik Yapı Malzemesi Olarak Tuğla ve Kiremit: Boğsak Adası Bizans Yerleşimi Örnekleme. *Sanat ve Tasarım Dergisi*, 141–162. <https://doi.org/10.18603/sanatvetasarim.370745>
- European Standards. (2015). *BS EN 772-1:2011+A1:2015 Methods of test for masonry units Determination of compressive strength*.
- Fernandes, F. M., Lourenço, P. B., & Castro, F. (2010). Ancient Clay Bricks: Manufacture and Properties. *Materials, Technologies and Practice in Historic Heritage Structures*, 29–48. https://doi.org/10.1007/978-90-481-2684-2_3
- Foss, C. (1979). *Ephesus After Antiquity: A Late Antique*. Cambridge University Press.
- Gadsden, J. A. (1975). *Infrared Spectra of Minerals and Related Inorganic Compounds*. Butterworths.
- Gerharz, R. R., Lantermann, R., & Spennemann, D. (1988). Munsell color charts: A necessity for archaeologists? *Australian Historical Archaeology*, 6, 88–95. <https://www.jstor.org/stable/29543213>
- Gliozzo, E. (2020). Ceramic technology. How to reconstruct the firing process. *Archaeological and Anthropological Sciences*, 12(11), 260. <https://doi.org/10.1007/s12520-020-01133-y>
- Hazinedar Coşkun, T. (2021). Kuşadası, Kadıkalesi Kazısı'nın 2017–2020 Sezonlarına Ait Bizans Cam Örnekleri. *Sanat Tarihi Dergisi*, 30(2), 1019–1037.
- Helen, T. (1975). *Organization of Roman brick production in the first and second centuries A.D.: an interpretation of Roman brick stamps*. Suomalainen Tiedeakatemia.
- Hlavay, J., Jonas, K., Elek, S., & Inczedy, J. (1978). Characterization of the Particle Size and the Crystallinity of Certain

- Minerals by IR Spectrophotometry and Other Instrumental Methods - 2. Investigations on Quartz and Feldspar. *Clays and Clay Minerals*, 26, 139–143. <https://doi.org/10.1346/CCMN.1978.0260209>
- İspir, M. (2010). *A Comprehensive Experimental Research on the Behaviour of Historical Brick Masonry Walls of 19th Century Buildings*. Unpublished PhD Thesis, Istanbul Technical University.
- Ion, R. M., Dumitriu, I., Fierascu, R. C., Ion, M. L., Pop, S. F., Radovici, C., Bunghez, R. I., & Niculescu, V. I. R. (2011). Thermal and mineralogical investigations of historical ceramic: A case study. *Journal of Thermal Analysis and Calorimetry*, 104(2), 487–493. <https://doi.org/10.1007/s10973-011-1517-6>
- Kahya, Y. (1992). *Istanbul Bizans Mimarisinde Kullanılan Tuğlaların Fiziksel ve Mekanik Özellikleri* [Doctoral Thesis]. Unpublished PhD Thesis, Istanbul Technical University.
- Kanmaz, M. B., & Ipekoğlu, B. (2016). Antik Kentlerde Deprem Sonrası Yapılan Onarımlar: Anaia Bizans Kilisesi. *Kargir Yapılarda Koruma ve Onarım Semineri VIII Conference Proceedings*, 8, 189–205.
- Kazancı, N., Dündar, S., Alçiçek, M. C., & Gürbüz, A. (2009). Quaternary deposits of the Büyük Menderes Graben in western Anatolia, Turkey: Implications for river capture and the longest Holocene estuary in the Aegean Sea. *Marine Geology*, 264(3–4), 165–176. <https://doi.org/10.1016/j.margeo.2009.05.003>
- Kretz, R. (1983). Symbols for rock-forming minerals. *American Mineralogist*, 68, 277–279.
- Kumar Mishra, A., Mishra, A., & Anshumali. (2021). Geochemical Characterization of Bricks Used in Historical Monuments of 14–18th Century CE of Haryana Region of the Indian Subcontinent: Reference to Raw Materials and Production Technique. *Construction and Building Materials*, 269, 121802. <https://doi.org/10.1016/j.conbuildmat.2020.121802>
- Kurugöl, S., & Tekin, Ç. (2010). Anadolu'da Bizans Dönemi kale Yapılarında Kullanılan Tuğlaların Fiziksel, Kimyasal ve Mekanik Özelliklerinin Değerlendirilmesi. *Journal of the Faculty of Engineering and Architecture of Gazi University*, 25(4), 767–777.
- Lopez-Arce, P., & Garcia-Guinea, J. (2005). Weathering traces in ancient bricks from historic buildings. *Building and Environment*, 40(7), 929–941. <https://doi.org/10.1016/j.buildenv.2004.08.027>
- Malacrino, C. G. (2010). *Constructing the Ancient World: Architectural Techniques of the Greeks and Romans*. Getty Publications.
- Mango, C. A. (1985). *Byzantine architecture*. Electa Editrice.
- Maniatis, Y., & Tite, M. S. (1981). Technological Examination of Neolithic-Bronze Age Pottery from Central and Southeast Europe and from the Near East. *Journal of Archaeological Science*, 8(1), 59–76. [https://doi.org/10.1016/0305-4403\(81\)90012-1](https://doi.org/10.1016/0305-4403(81)90012-1)
- Maritan, L., Nodari, L., Mazzoli, C., Milano, A., & Russo, U. (2006). Influence of Firing Conditions on Ceramic Products: Experimental Study on Clay Rich in Organic Matter. *Applied Clay Science*, 31(1–2), 1–15. <https://doi.org/10.1016/j.clay.2005.08.007>
- Mercangöz, Z. (2005). 4. Yılında Kuşadası, Kadıkalesi/Anaia Kazısı. *Sanat Tarihi Dergisi*, XIV–1, 205–223.
- Mercangöz, Z. (2007). Emporion ve kommerkion olarak anaia'nın değişken tarihsel yazgısı. *On İkinci ve On Üçüncü Yüzyıllarda Bizans Dünyasında Değişim, I. Uluslararası Sevgi Gönül Bizans Araştırmaları Sempozyumu / First International Sevgi Gönül Byzantine Studies Symposium, Bildiriler/ Proceedings, 25-28 June 2007*, 279–292.
- Mercangöz, Z. (2013). Archaeological Finds on Late Byzantine Commercial Productions at Kadıkalesi, Kuşadası. In Z. Mercangöz (Ed.), *Byzantine Craftsmen - Latin Patrons* (pp. 25–58).
- Mercangöz, Z., & Tok, E. (2011). Kuşadası kadıkalesi 2010 kazı sezonu çalışmaları. 33. *Kazı Sonuçları Toplantısı-2, 23-28 May 2011, Ministry of Culture and Tourism, Ankara*, 353–372.
- Moorey, P. R. S. (1999). *Ancient Mesopotamian Materials and Industries: The Archaeological Evidence*. Eisenbrauns.
- Moropoulou, A., Bakolas, A., & Bisbikou, K. (1995). Thermal Analysis as a Method of Characterizing Ancient Ceramic Technologies. *Thermochimica Acta*, 2570, 743–753.
- Moropoulou, A., Çakmak, A., & Polikreti, K. (2002). Provenance and Technology Investigation of Agia Sophia Bricks, Istanbul, Turkey. *Journal of the American Ceramic Society*, 85(2), 366–372.
- MTA. (2002). *Türkiye jeoloji haritası / Geological map of Turkey (Denizli)*. Retrieved March 2, 2023. <https://www.mta.gov.tr/v3.0/sayfalar/hizmetler/doc/DENIZLZL.pdf>
- Munsell Color (Firm). (2000). *Munsell Soil Color Charts: year 2000 revised washable edition*. GretagMacbeth, Munsell Color.
- Oguz, C., Turker, F., & Kockal, N. U. (2014). Construction materials used in the historical roman era bath in Myra. *Scientific World Journal*, 2014. <https://doi.org/10.1155/2014/536105>
- Ousterhout, R. (1999). *Master Builders of Byzantium*. Princeton University Press.
- Özyıldırım, M., & Akyol, A. A. (2016). Olba Tuğla Örneği: Arkeolojik ve Arkeometrik Yaklaşım. *Seleucia*, 6, 395–411.
- Paama, L., Pitkänen, I., & Perämäki, P. (2000). Analysis of archaeological samples and local clays using ICP-AES, TG-DTG and FTIR techniques. *Talanta*, 51(2), 349–357. [https://doi.org/10.1016/S0039-9140\(99\)00281-7](https://doi.org/10.1016/S0039-9140(99)00281-7)
- Pavia, S. (2006). The Determination of Brick Provenance and Technology Using Analytical Techniques from the Physical Sciences. *Archaeometry*, 48(2), 201–218.
- Pérez-Monserrat, E. M., Causarano, M., Maritan, L., Chavarria, A., Pietro, G., & Cultrone, G. (2022). Roman brick production technologies in Padua (Northern Italy) along the Late Antiquity and Medieval Times: Durable bricks on high humid envions. *Journal of Cultural Heritage*, 54, 12–20. <https://doi.org/10.1016/j.culher.2022.01.007>
- Pérez-Monserrat, E. M., Maritan, L., Garbin, E., & Cultrone, G. (2021). Production Technologies of Ancient Bricks from Padua, Italy: Changing Colors and Resistance over Time. *Minerals*, 11(7). <https://doi.org/10.3390/min11070744>
- Ramachandran, V. S., Paroli, R. M., Beaudoin, J. J., & Delgado, A. H. (2002). 12 - Clay-Based Construction Products. In V. S. Ramachandran, R. M. Paroli, J. J. Beaudoin, & A. H.

- Delgado (Eds.), *Handbook of Thermal Analysis of Construction Materials* (pp. 491–530). William Andrew Publishing. <https://doi.org/10.1016/B978-081551487-9.50014-1>
- Rathossi, C., & Pontikes, Y. (2010). Effect of firing temperature and atmosphere on ceramics made of NW Peloponnese clay sediments. Part I: Reaction paths, crystalline phases, microstructure and colour. *Journal of the European Ceramic Society*, 30(9), 1841–1851. <https://doi.org/10.1016/j.jeurceramsoc.2010.02.002>
- Riccardi, M. P., Messiga, B., & Duminuco, P. (1999). An Approach to the Dynamics of Clay Firing. *Applied Clay Science*, 15, 393–409.
- RILEM. (1980). Essais recommandés pour mesurer l'altération des pierres et évaluer l'efficacité des méthodes de traitement / Recommended tests to measure the deterioration of stone and to assess the effectiveness of treatment methods. *Materials and Construction*, 13(73), 175–253.
- Scalenghe, R., Barello, F., Saiano, F., Ferrara, E., Fontaine, C., Caner, L., Olivetti, E., Boni, I., & Petit, S. (2015). Material sources of the Roman brick-making industry in the I and II century A.D. from Regio IX, Regio XI and Alpes Cottiae. *Quaternary International*, 357, 189–206. <https://doi.org/10.1016/j.quaint.2014.11.026>
- Scatigno, C., Prieto-Taboada, N., Preite Martinez, M., Conte, A. M., & Madariaga, J. M. (2018). A Non-Invasive Spectroscopic Study to Evaluate Both Technological Features and Conservation State of Two Types of Ancient Roman Coloured Bricks. *Spectrochimica Acta - Part A: Molecular and Biomolecular Spectroscopy*, 204, 55–63. <https://doi.org/10.1016/j.saa.2018.06.023>
- Scherer, G. W. (1999). Crystallization in pores. *Cement and Concrete Research*, 29(8), 1347–1358. [https://doi.org/10.1016/S0008-8846\(99\)00002-2](https://doi.org/10.1016/S0008-8846(99)00002-2)
- Şerifaki, K. (2017). *Determination of Byzantine Wall Painting Techniques in Western Anatolia* [Doctoral Thesis]. Unpublished PhD Thesis, Izmir Institute of Technology.
- Singh, P., & Sharma, S. (2016). Thermal and spectroscopic characterization of archeological pottery from Ambari, Assam. *Journal of Archaeological Science: Reports*, 5, 557–563. <https://doi.org/10.1016/j.jasrep.2016.01.002>
- Stefanidou, M., Papayianni, I., & Pacht, V. (2015). Analysis and characterization of Roman and Byzantine fired bricks from Greece. *Materials and Structures/materiaux Et Constructions*, 48(7), 2251–2260. <https://doi.org/10.1617/s11527-014-0306-7>
- Stuart, B. H. (2007). Molecular Spectroscopy. In *Analytical Techniques in Materials Conservation* (pp. 109–208). John Wiley & Sons, Ltd. <https://doi.org/10.1002/9780470060520.CH4>
- Stubňa, I., & Podoba, R. (2013). Romanesque and Gothic Bricks from Church in Pác - Estimation of the Firing Temperature. *Epitoanyag-Journal of Silicate Based and Composite Materials*, 65, 48–51.
- Taranto, M., Barba, L., Blancas, J., Bloise, A., Cappa, M., Chiaravallotti, F., Crisci, G. M., Cura, M., De Angelis, D., De Luca, R., Lezzerini, M., Pecci, A., & Miriello, D. (2019). The bricks of Hagia Sophia (Istanbul, Turkey): A new hypothesis to explain their compositional difference. *Journal of Cultural Heritage*, 38, 136–146. <https://doi.org/10.1016/j.culher.2019.02.009>
- Tarhan, İ., & Işık, İ. (2020). An In-depth Chemometric Study: Archaeometric Characterization of Ceramic Shards Excavated from the Sanctuary of Hecate at Lagina in Muğla (Turkey) by FTIR Spectroscopy and Multivariate Data Analysis. *Vibrational Spectroscopy*, 111(September). <https://doi.org/10.1016/j.vibspec.2020.103172>
- Tekin, Ç., & Kurugöl, S. (2011). Physicochemical and Pozzolan Properties of the Bricks Used in Certain Historic Buildings in Anatolia. *Gazi University Journal of Science*, 24(4), 2011.
- Tepe, Ç., Sözbilir, H., Eski, S., Sümer, Ö., & Özkaymak, Ç. (2021). Updated historical earthquake catalog of İzmir region (Western Anatolia) and its importance for the determination of seismogenic source. *Turkish Journal of Earth Sciences*, 30(8), 779–805. <https://doi.org/10.3906/yer-2101-14>
- Tucci, P. L. (2015). The Materials and Techniques of Greek and Roman Architecture. In *The Oxford Handbook of Greek and Roman Art and Architecture* (pp. 241–265). Oxford University Press.
- Uğurlu Sağın, E. (2017). Anadolu'da Roma Dönemi Yapı Tuğlalarının Özellikleri. *Journal of the Faculty of Engineering and Architecture of Gazi University*, 32(1), 227–236. <https://doi.org/10.17341/gazimmfd.300612>
- Uğurlu Sağın, E., & Böke, H. (2013). Characteristics of bricks used in the domes of some historic bath buildings. *Journal of Cultural Heritage*, 14(3 SUPPL), 73–76. <https://doi.org/10.1016/j.culher.2012.11.030>
- Ulukaya, S., Yoruç, A. B. H., Yüzer, N., & Oktay, D. (2017). Material characterization of byzantine period brick masonry walls revealed in Istanbul (Turkey). *Periodica Polytechnica Civil Engineering*, 61(2), 209–215. <https://doi.org/10.3311/PPci.8868>
- Valanciene, V., Siauciuonas, R., & Baltusnikaite, J. (2010). The influence of mineralogical composition on the colour of clay body. *Journal of the European Ceramic Society*, 30(7), 1609–1617. <https://doi.org/10.1016/j.jeurceramsoc.2010.01.017>
- Wang, S., Gainey, L., Mackinnon, I. D. R., Allen, C., Gu, Y., & Xi, Y. (2023). Thermal behaviors of clay minerals as key components and additives for fired brick properties: A review. *Journal of Building Engineering*, 66, 105802. <https://doi.org/10.1016/J.JOBE.2022.105802>
- Warr, L. N. (2020). Recommended abbreviations for the names of clay minerals and associated phases. *Clay Minerals*, 55(3), 261–264. <https://doi.org/10.1180/CLM.2020.30>
- Whitney, D. L., & Evans, B. W. (2010). Abbreviations for names of rock-forming minerals. *American Mineralogist*, 95, 185–187. <https://doi.org/10.2138/am.2010.3371>
- Wright, G. R. H. (2005). *Ancient Building Technology, Volume 2: Materials (2 Vols)*. Brill.
- Wright, G. R. H. (2009). *Ancient Building Technology, Volume 3: Construction (2 vols)*. Brill.

Springer Nature or its licensor (e.g. a society or other partner) holds exclusive rights to this article under a publishing agreement with the author(s) or other rightsholder(s); author self-archiving of the accepted manuscript version of this article is solely governed by the terms of such publishing agreement and applicable law.